

Catalytic Layer Location in MEA and Air Supply Influence on The Performance of an Open-Cathode Direct Ethanol Fuel Cell

D. A. Moreno J, Daniella E. Pacheco C., L. C. Ordóñez^{*}

Centro de Investigación Científica de Yucatán, A.C Unidad de Energía Renovable, Centro de Investigación Científica de Yucatán, C. 43 No. 130
Col. Chuburná de Hidalgo, Mérida, Yucatán, 97200. México. Tel +52-999-9428330, e-mail: leol@cicy.mx

ABSTRACT

The influence of the catalytic layer location on the performance of an open-cathode Direct Ethanol Fuel Cell (DEFC) was investigated using three different methods of preparation of the membrane electrode assembly (MEA). A catalytic load of 1 mgPtcm^{-2} of a commercial catalysts of PtRu/C was used in both anode and cathode electrodes. In MEA 1, catalyst layers (CL) were deposited directly onto the Nafion® membrane surface. MEA 2 consisted of two CL's: an inner, placed on the member surface and an outer CL located onto the carbon cloth diffuser layer (DL). MEA 3 was prepared using Pt-Black as the inner CL and PtRu/C or PtSn/C as the outer CL. Additionally we report two approaches for the operation of the open-cathode DEFC: air-self breathing (ASB) and forced-air convection (FAC). The combination of the inner and outer CL improved cell performance. The best activity was recorded with the outer CL prepared with PtSn/C catalyst. There is a strongly dependence between air supply to the cathode and cell performance. Our Open-Cathode DEFC design showed a decrease of 24.6 % of the power density in air-self breathing operation with respect to forced-air convection at RT.

Keywords: DEFC, Open-Cathode design, MEA preparation



1. Introduction

Direct ethanol fuel cells (DEFCs) are attractive power source devices since alcohols can be easily handled, transported and stored using the existing infrastructure. On the other hand, ethanol is available from biomass fermentation, it is not as toxic as methanol, it presents lower permeation rates through Nafion® membranes probably by its larger molecular size [1] and, it has a higher energy density than methanol [2]. One of the most important challenges to achieve the DEFC portability is avoiding the oxygen feeding from heavy tanks or air pumps. . An alternative is to consider open-cathodes designs that allow the operation with oxygen from air. There are two operational approaches for DEFC usage with open cathodes [3]:

- Air-self breathing (ASB): it takes oxygen from the air by natural convection [4].
- Forced-air convection (FAC): It uses fans at the cathode edge to force the air convection into the cathode [3].

The air-self breathing approach is very attractive since parasitic loads by external devices are minimized. But this type of operation reduces the overall performance of the fuel cell since the oxygen diffusion by natural convection is slow[4]. On the other hand the forced-air convection approach gives a higher cell performance [5]. However this type of architecture requires tight control of the air flow since its excess could reduce the average temperature of the stack causing a decrease in the electrochemical reaction rate [6]. A good performance of an open-cathode design requires an optimal architecture in the field of the flow channels and the Membrane electrode assembly (MEA) design. and: The improvement of MEA performance depends on its components and the assembly process [7]. In all cases, the MEA manufacture must consider the optimal interaction between the reactants (liquid or gas), the catalytic site and the electrolyte.

There are two basic methods for the assembly process,: a) the deposition of the catalyst layer on the DL followed by the addition or hot pressing to the membrane and b) deposition of catalyst layer directly onto the membrane surface followed by the addition or hot pressing of the DL [8], this process is called catalyst-coated membrane (CCM).

Due to the importance of the MEA manufacture on the global efficiency of the open-cathode ethanol fuel cell, we constructed an open-cathode DEFC and studied the influence of the catalytic layer location on its performance. Three different methods for MEA preparation were investigated: a) Depositing catalyst layers (CL) directly on the membrane surface, b) using two CLs, an inner layer placed on the member surface and an outer CL located onto the carbon cloth diffuser (DL) and c) using Pt-Black as the inner CL and PtRu/C or PtSn/C as the outer CL, which presented best performance. Results also showed that the air supply to the cathode plays an important role in the performance of the Open-Cathode DEFC design

2. Experimental

2.1. Materials

In all experiments Nafion® 117 membranes (DuPont) were used as a polymer electrolyte. We followed a three steps procedure to remove organic materials and activate the membranes consisting on: boiling in 3% H₂O₂ solution for 45 min; boiling in 1 M H₂SO₄ for 45 minutes and washing in de-ionized water.

The catalytic materials used were Pt_{0.2}Ru_{0.1}/C HiSPEC™ 5000 (Alfa Aesar), Pt-Black (Alfa Aesar) and PtSn/C (Pt:Sn, 1:1) 50 wt % prepared in our laboratory. Carbon cloth EC-CC1 (ElectroChem Inc) was used as DL. Graphite-polymer compose was used as anode and cathode plates for the single cell (table 1).



Table 1. Graphite-polymer compose properties

Density	1.82 gcm ⁻³
Tensile modulus at 25 °C	17000 MPa
Electrical conductivity	50 ± 10 S/cm
Thermal conductivity at 25 °C	15.8 W m ⁻¹ K ⁻¹

2.2. Synthesis of PtSn/C

The carbon-supported PtSn electrocatalyst 50 wt % (Pt:Sn, 1:1, atomic ratio) was synthesized using sodium borohydride reduction method. Pt salt (H₂PtCl₆, Aldrich) and Sn salt (SnCl₄, Aldrich) were used as precursors for the catalyst. Carbon Vulcan XC-72 was ultrasonically dispersed by 30 minutes in a three neck volumetric flask with 50/50 % v/v 2-propanol/de-ionized water solution. Then, appropriate amounts of Pt salt and Sn salt were added to the dispersed carbon. The mixture was stirred in a reflux system for 3 hours at room temperature, then appropriate amount of NaBH₄ solution was added drop by drop to the mixture and stirred for 6 h. The obtained slurry was filtered, washed and dried in a vacuum oven at 80 °C overnight. Finally, the catalyst was thermal treated at 200 °C for 2 h in a nitrogen atmosphere.

2.3. MEA preparation

The catalytic ink was composed of the catalyst (Pt-black, PtRu/C or PtSn/C) with ionomer solution (5 % w/w, Alfa Aesar) and 2-propanol. This dispersion was sonicated for 30 minutes to get a homogeneous ink. The deposition of the catalytic ink was carried out by brush painting method at different locations in the MEA. For the comparison, all MEAs have 9 cm² of active area with a catalyst load of 1 mgPtcm⁻² in anode and cathode electrodes.

2.3.1. MEA-1

Commercial PtRu/C catalyst was used in anode and cathode electrodes. The catalytic load was 1mgPtcm⁻². Catalytic ink was deposited directly on both sites of the membrane surface at 60 °C. After that, a 9 cm² piece of carbon cloth was placed over each catalytic layer and finally the MEA was assembled into the cell.

2.3.2. MEA-2

Two CL's of PtRu/C were deposited on anode and cathode electrodes: an inner CL with a catalytic load of 0.5 mgPtcm⁻² was painted directly onto membrane surface like in MEA-1. Next, an outer CL with total catalytic load of 0.5 mgPtcm⁻² was coated onto the carbon cloth diffuser (DL). Finally the electrodes were assembly by hot-pressing at 201 kgcm⁻² for 9 minutes at 120 °C. Total catalytic load was 1mgPtcm⁻² in anode and cathode.

2.3.3. MEA-3

Two CL's were deposited in anode and cathode electrodes similar to MEA-2. But in this case, in the anode side two different CL's with 0.5mgPtcm⁻² were tested. The first one was composed by PtRu/C (MEA-3a) and the latter was composed by PtSn/C (MEA-3b). Finally, the electrodes were assembled by hot-pressing at 50 kgcm⁻² for 1 minute at 130 °C.



2.4. Open-cathode fuel cell design

All experiments were performed in an Open-Cathode DEFC designed at our laboratory figure 1a and 1b show the anode and cathode designs respectively. The anode flow field is a single-serpentine pattern. The cathode design is a rhomboid array that facilitates water removal and suitable air convection into the cell. The cathode side has an electrical surface contact area of 61 %. In both electrodes the active area is 9 cm².

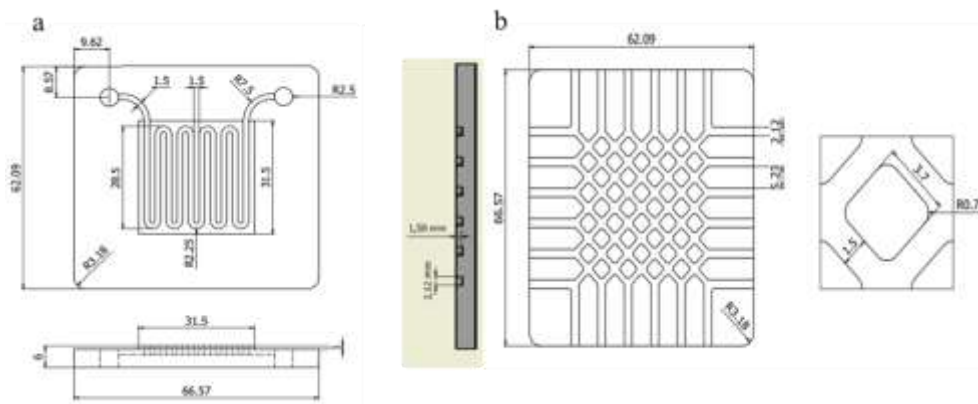


Fig 1. Open-Cathode DEFC design: a) anode mono-polar plate, b) cathode mono-polar plate

2.5. Cell performance test

The electrochemical measurements were performed in a potentiostat/galvanostat AutoLab PGSTAT302. Before testing the cell, all MEAs were activated by heating the cell at 60 °C and passing de-ionized water through the anode side for 3 hours at 1.5 mL/min to ensure suitable humidification of the membrane. Next, 1M ethanol solution was fed to the anode at 1.5 mL/min. A chronoamperometry measurement was carried out at 0.1 V for 1800 seconds. At this step, the current was recorded to find a point very close to the limiting current of the cell. Then, a chronopotentiometry measurement was performed to hold the current, at the point recorded before, during 1800 seconds. This procedure was performed until the fuel cell presented a stable signal. After activation, polarization curves were registered using scan rates of 5 and 10 mVs⁻¹ at 25 °C and 60 °C. In both temperatures, the cell was tested in air-self breathing (ASB) and forced-air convection (FAC) mode to measure the air supply influence on the cell performance. Electrochemical impedance spectroscopy (EIS) analysis was carried out to understand the mass transport process, ohmic and charge transfer resistance. The galvanostatic impedance spectra were obtained at a frequency range between 3 kHz and 0.1 Hz at a constant current, very close to the limiting current in the mass transport zone of polarization curve. We tested 50 points, and sinusoidal current amplitude of signal around 6 % of the constant current setting. The potentiostatic impedance spectra were obtained at a frequency range of 250 kHz-0.01 Hz and 25 kHz-0.1 Hz according to the response of each MEA. We used 50 points and sinusoidal voltage amplitude of 0.005 V, in all cases at open circuit potential (OCP).



3. Results and discussion

3.1. MEA-1, MEA-2 and MEA-3a

Three MEAs with different catalytic layer location were tested under the same conditions. Figure 2 shows the comparison of the polarization curves registered for the three MEAs at 60 °C. It can be observed that the OCP is very similar in MEA-1 and MEA-2 (0.34 V and 0.36 V respectively). However, the current and power densities increase with the utilization of two catalytic layers. This could be attributed to the lower ohmic resistance in the assembly as can be seen in the table 2. MEA-1 has $11.7 \Omega\text{cm}^2$ and MEA-2 has $2.61 \Omega\text{cm}^2$. This decrease in ohmic resistance of the assembly implies a better contact between the diffusion layer, catalytic layer and membrane.

Hot-pressing helps to reduce the resistance in the assembly in comparison with not hot-pressing electrodes as observed in MEA-2.

As observed in figure 2, the best performance was recorded with MEA-3a which has an inner unsupported Pt catalyst layer. In this case, OCP and current density is higher (0.46 V and 11 mAcm^{-2} respectively) than in MEA-1 and MEA-2.

According with Chien-Hao *et al.* [9] the inner catalyst layer helps to reduce the ethanol crossover since catalysts particles deposited onto membrane acts as ethanol barrier. Probably the MEA-3a behavior could be related to a reduction of ethanol crossover. However, the ethanol crossover measurement is technically difficult to perform with the open-cathode design because a nitrogen inert atmosphere at cathode is needed. Nevertheless it is clear that there is an improvement in the MEA performance by using two catalyst layers.

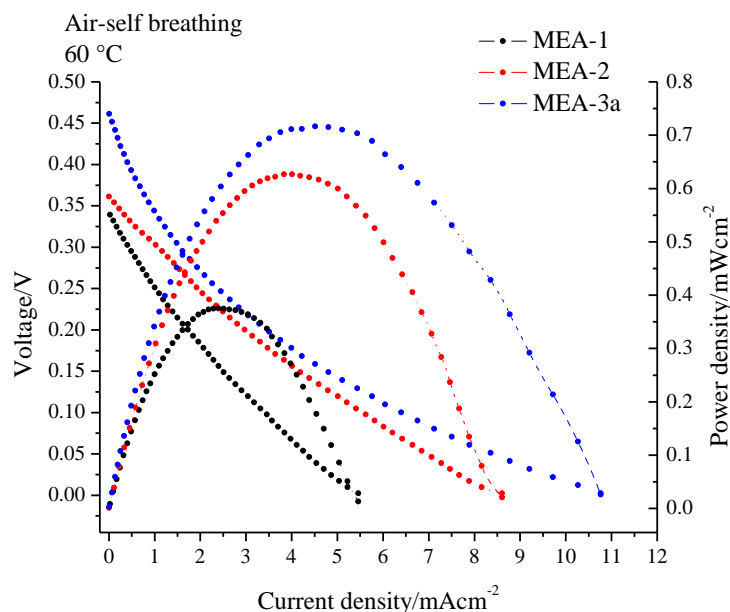


Fig 2. Polarization curves and density power for MEA-1, MEA-2, MEA-3a: ASB mode, scan rate of 10 mVs⁻¹. Fuel: 1 M ethanol solution. Operation temperature of 60 °C



Table 2. Ohmic resistances determinated by Potentiostatic EIS.

MEA	Ohmic resistance/ Ωcm^2
MEA-1	11.7
MEA-2	2.61
MEA-3a	1.5

3.2. MEA-3a and MEA-3b: catalyst performance and air supply influence

PtSn/C and PtRu/C catalysts were deposited in the outer layer in order to test their influence in the MEA performance. The PtSn/C presented the best activity for ethanol oxidation reaction (EOR) [9, 10]. Figure 3 and figure 4 show the polarization curves and power density of the MEA-3a and MEA-3b at 25 °C and 60 °C respectively. In both cases, air-self breathing (ASB) and Forced-air convection (FAC) mode were tested using a scan rate of 5 mVs⁻¹ and 1M ethanol solution. It can be seen that the OCP at 25 °C is higher with PtSn/C synthesized in our laboratory in comparison with the commercial PtRu/C material. At 25 and 60 °C the limiting current density and power density are higher using PtSn/C than with PtRu/C. This increase on the power density is 68.8% in ASB mode and 74.6% in FAC at 25 °C. These results are important since they could imply higher efficiency in portable applications. On the other hand we observed dependence between air supply and performance of the cell.

MEA-3b, which showed the best performance, presented a reduction in the peak of power density between the operation in FAC vs ABS mode, being 23.8% at 25°C and 34.5% at 60°C as observed in figure 4. Considering the several advantages related to parasitic losses by external devices at ASB operation, our open-cathode fuel cell has relative low decrease and it could be operated with suitable performance in ASB mode in comparison with FAC.

Table 3 presents the different power densities of the MEAs in ASB and FAC mode at 25 °C and 60 °C. The highest peak of power density is 3.21 mWcm⁻² recorded at 60 °C with the MEA-3b in FAC mode. The increment on the performance with forced air supply is mostly related to a charge transfer effect than to the ohmic resistance affect, since the potentiostatic EIS spectra (table 4) shows no significant variations on the ohmic resistance between the two operation approaches, especially at 25 °C. Instead, at 60 °C, the ohmic resistance slightly increased, probably due to membrane dehydration caused by airflow. However, the forced-air convection mode helps to improve the oxygen diffusion and it has the strongest influence on the charge transfer resistance and performance of the cell. From galvanostatic EIS spectra at 60 °C (Fig. 5) it can be seen that the charge transfer resistance goes down with the increment on the air supply flux in MEA-3a and MEA-3b. The lowest charge transfer resistances was recorded in the MEA-3b, this agrees with the best performance in terms of power and current densities. Table 5, shows the values of ohmic and resistance to the charge transfer (RCT) obtained by galvanostatic EIS at 60 °C. as well as the influence of air supply on the RCT that cause a reduction from 37 Ωcm^2 to 26 Ωcm^2 in MEA-3a and from 23 Ωcm^2 to 17 Ωcm^2 in MEA-3b. The improved activity of MEA containing the PtSn/C catalyst could be explained by a reduction in the RCT. The impedance values were obtained using “electrochemical circle fit” in NOVA 1.9 considering the follow equivalent circuit: (R1+ CPE/R2) where R1 is related with the ohmic resistance, CPE is a constant phase element related with the capacitance of the double layer and R2 is the resistance to the charge transfer.



Table 3. Power density of MEA-3a and MEA-3b at 25 °C and 60 °C.

MEAs	Power density in ASB/ mWcm ⁻²	Power density in FAC/ mWcm ⁻²	Temperature °C
MEA-3a	0.3	0.32	25
MEA-3b	0.96	1.26	25
MEA-3a	0.72	1.13	60
MEA-3b	2.1	3.21	60

Table 4. Potentiostatic EIS: ohmic resistance for MEA-3a and MEA-3b.

MEAs	Constant potential (V) ASB/FAC	Ohmic resistance Ωcm ² / ASB	Ohmic resistance Ωcm ² / AFC	Temperature/°C
MEA-3a	0.46/0.52	1.6	1.6	25
MEA-3b	0.63	1.3	1.3	25
MEA-3a	0.46/0.57	1.5	1.9	60
MEA-3b	0.63	1.08	1.5	60

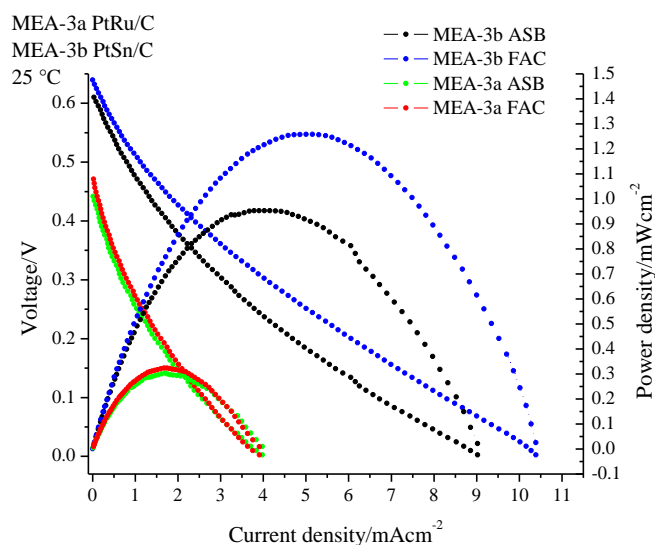


Fig 3. Polarization curves and density power for MEA-1, MEA-2, MEA-3a: ASB mode, scan rate of 10 mVs⁻¹. Fuel: 1M ethanol solution. Operating temperature of 60 °C.



Table 5. Galvanostatic EIS: ohmic and charge transfer resistance (RCT) for MEA-3a and MEA-3b.

MEAs	R ohmic (Ωcm^2) ASB/FAC	RCT (Ωcm^2) ASB	RCT (Ωcm^2) FAC	Constant Current(A) ASB/FAC	Temperature °C
MEA-3a	1.62/1.71	-	161	0.03/0.03	25
MEA-3b	1.2/1.4	-	38.7	0.07/0.07	25
MEA-3a	1.57/1.9	37	26	0.07/0.11	60
MEA-3b	1.1/1.6	23	17	0.19/0.27	60

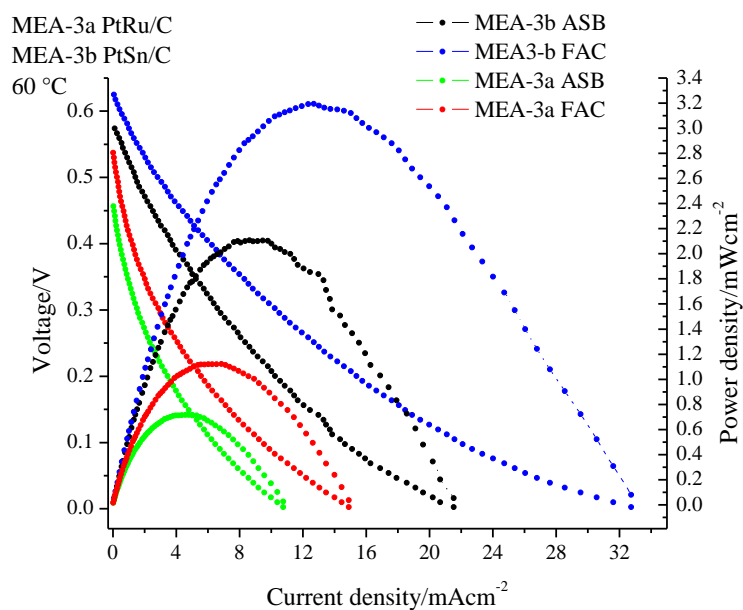


Fig 4. Polarization curves and density power for MEA-3a and MEA-3b: ASB mode, scan rate of 10 mVs^{-1} . Fuel: 1M ethanol solution. Operating temperature of 60°C .



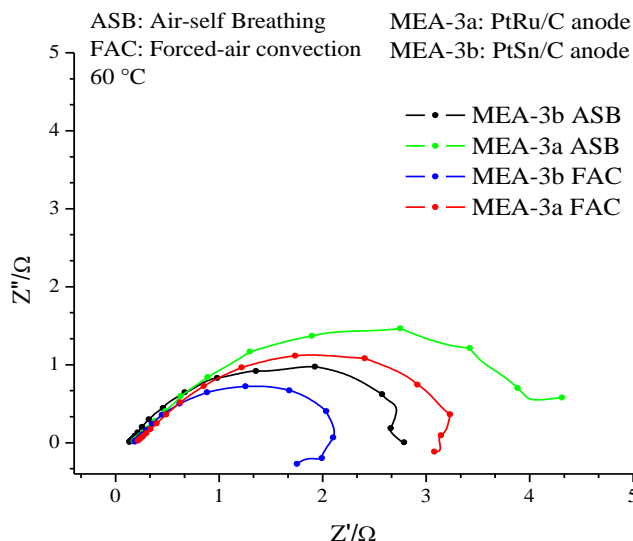


Fig 5. Galvanostatic EIS spectra for MEA-3a and MEA-3b in ASB and FAC mode at 60 °C, frequency range of 3 kHz to 0.1 Hz in mass transfer zone of polarization curve.

4. Summary and perspectives

The influence of the catalytic layer location and air supply on the performance was determined by testing three different MEA-preparation methods and two operational open-cathode approaches. It was observed that the ohmic resistance is affected by the assembly method, in MEA-1 and MEA-2, since a better contact between DL, CL and membrane gives lower ohmic resistances. In this case, the utilization of two catalytic layers, an inner directly deposited onto the Nafion membrane surface and an outer catalyst layer deposited onto the DL, helps to improve the contact resistance generating higher power and current densities. Additionally, the use of unsupported Pt inner catalyst layer shows a significant increment on the OCP, probably by decreasing the rate of ethanol crossover due to the Pt particles acting as a reactive ethanol filter. The use of PtSn/C on the catalyst layer presented better performance than PtRu/C. This is explained by an important increment on the OCP, current and power density mostly related to a lower resistance to the charge transfer. The air supply to the cathode also has an important impact on the cell performance. The FAC helps to improve the oxygen diffusion and increases the power and current densities. According to the test with MEA-3b, the difference in the power density between the operation in ASB and FAC is 23.8 % at 25 °C and 34.5 % at 60 °C. Considering that ASB operation does not have parasitic losses by external devices, our open-cathode fuel cell has a relatively low power density decrease and it could be considered as a promising portable power supply.



Acknowledgements

The authors express their gratitude to M. C. Enrique Escobedo Hernández and Ing. Romeo Moreno for his collaboration in DEFC tests, Ing. Gustavo Martínez and Dra. Ana Valenzuela for technical support. The authors acknowledge the financial support for this work from FOMIX-Quintana Roo with the project 175119. D. A. Moreno thank to CONACYT for grant No. 280971.

References

1. Song, S. and P. Tsiakaras, Recent progress in direct ethanol proton exchange membrane fuel cells (DE-PEMFCs). *Applied Catalysis B-Environmental*, 2006, 63(3): p. 187-193.
2. Ekdharmasuit, P., A. Therdthianwong, and S. Therdthianwong, Anode structure design for generating high stable power output for direct ethanol fuel cells. *Fuel*, 2013, 113(0): p. 69-76.
3. Liu, W., et al., Experimental study of proton exchange membrane fuel cells using Nafion 212 and Nafion 211 for portable application at ambient pressure and temperature conditions. *International Journal of Hydrogen Energy*, 37(5): p. 4673-4677.2012
4. Bussayajarn, N., et al., Planar air breathing PEMFC with self-humidifying MEA and open cathode geometry design for portable applications. *International Journal of Hydrogen Energy*, 34(18): p. 7761-7767.2009
5. Dhathathreya, K.S., et al., Forced Air-Breathing PEMFC Stacks. *International Journal of Electrochemistry*, 2012: p. 7.2012
6. Barreras, F., et al., Experimental study of the pressure drop in the cathode side of air-forced Open-cathode proton exchange membrane fuel cells. *International Journal of Hydrogen Energy*, 36(13): p. 7612-7620.2011
7. Wu, B., et al., The performance improvement of membrane and electrode assembly in open-cathode proton exchange membrane fuel cell. *International Journal of Hydrogen Energy*, 2013, 38(25): p. 10978-10984.
8. Mehta, V. and J.S. Cooper, Review and analysis of PEM fuel cell design and manufacturing. *Journal of Power Sources*, 114(1): p. 32-53.2003
9. Wan, C.-H. and C.-L. Chen, Mitigating ethanol crossover in DEFC: A composite anode with a thin layer of Pt50-Sn50 nanoparticles directly deposited into Nafion® membrane surface. *International Journal of Hydrogen Energy*, 34(23): p. 9515-9522.2009
10. Song, S.Q., et al., Direct ethanol PEM fuel cells: The case of platinum based anodes. *International Journal of Hydrogen Energy*, 30(9): p. 995-1001.2005

